'Extraneous proteins can protect oleosin from gastric digestion and so affect the 'oil body' size in the small intestine. '

Impact of extraneous proteins on the gastrointestinal fate of sunflower seed (*Helianthus annuus*) oil bodies: A simulated gastrointestinal tract study

Sakunkhun Makkhun[ab], Amit Khosla[b], Tim Foster[b],
David Julian McClements[c] Myriam M.L. Grundy[d] and David A. Gray*[b]

[a] **University of Phayao, Division of Food Science and Technology,**
School of Agriculture and Natural Resources, Muang, Phayao, Thailand. 56000

[b] **University of Nottingham, Division of Food Sciences, School of Biosciences,**
Sutton Bonington Campus, Leicestershire, England. LE12 5RD

[c] **Biopolymers and Colloids Research Laboratory, Department of Food Science,**
University of Massachusetts, Amherst, MA 01003, USA

[d]**King's College London, Department of Biochemistry, Diabetes & Nutritional Sciences Division,**
Franklin-Wilkins Building, London SE1 9NH

*Corresponding author address:

University of Nottingham, School of Biosciences,
Division of Food Sciences, Sutton Bonington Campus, Leicestershire LE12 5RD.
Tel: 00 44 (0)1159 516147. Fax: 00 44 (0)1159 516142. David.Gray@nottingham.ac.uk

72
73 The fate of oil body and protein enriched oil body during digestion under simulated gastrointestinal conditions
74 was studied.
75

76

Oil body   **Protein enriched oil body**
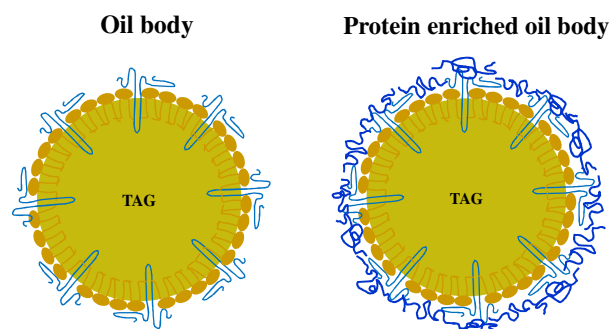
77

78

79 **Abbreviations:**

80 BCA   Bichinconinic acid

81 COB   Crude oil bodies

82 dH$_2$O   Deionized water

83 PL   Phospholipids

84 SDS   Sodium dodecyl sulphate

85 SDS-PAGE   Sodium dodecyl sulphate-polyacrylamide gel electrophoresis

86 TAG   Triacylglycerol

87 WOB   Washed oil bodies

88 WOB-SC   Sodium caseinate enriched oil bodies

89 WOB-WPI   Whey protein isolate enriched oil bodies

90 ζ-potential   Zeta potential

91

92 **Abstract**

93 In this study, we examined the physicochemical nature of sunflower seed oil bodies (in the absence and

94 presence of added protein) exposed to gastrointestinal conditions *in vitro:* crude oil bodies (COB); washed oil

95 bodies (WOB); whey protein isolate-enriched oil bodies (WOB-WPI); and, sodium caseinate enriched-oil

96 bodies (WOB-SC). All oil body emulsions were passed through an *in vitro* digestion model that mimicked the

97 stomach and duodenal environments, and their physicochemical properties were measured before, during, and

98 after digestion. Oil bodies had a positive charge under gastric conditions because the pH was below the

99 isoelectric point of the adsorbed protein layer, but they had a negative charge under duodenal conditions which

100 was attributed to changes in interfacial composition resulting from adsorption of bile salts. Oil bodies were

101 highly susceptible to flocculation and coalescence in both gastric and duodenal conditions. SDS-PAGE

102 analysis indicated degradation of oleosin proteins (ca. 18-21 kDa) to a greater or lesser extent (dependent on

103 the emulsion) during the gastric phase in all emulsions tested; there is evidence that some oleosin remained

104 intact in the crude oil body preparation during this phase of the digestion process. Measurements of protein

105 displacement from the surface of COBs during direct exposure to bile salts, without inclusion of a gastric

106 phase, indicated the removal of intact oleosin from native oil bodies.

107

108 **Keywords:** oil bodies; oleosomes; emulsions; bile salts; digestion

1. Introduction

The seeds of many plants species store oil as food reserves for germination, and for post germination growth of the seedlings, in organelles called oil bodies or oleosomes. Oil bodies are mainly composed of triacylglycerol (TAG) core surrounded by phospholipids (PL) and alkaline proteins, e.g. oleosins [1]. These proteins prevent coalescence of oil bodies in the cytosol of oilseed cells[2-6]. Furthermore, at neutral pH they have a net negative charge which prevents coalescence *ex vivo* when oil bodies are dispersed in a suspension. Oil bodies isolated from plant seeds in aqueous media are therefore a natural emulsion that may represent a vehicle to deliver stable, pre-emulsified oil into a range of food systems. In addition to their physical stability, oil bodies, ex-vivo, carry essential fatty acids and a number of lipophilic bioactives, such as vitamin E and oryzanols, depending on the parent seed [7-9]. Sunflower seed oil bodies were selected for this study as they have been well characterised by our group.

It is important that any delivery system is capable of delivering the encapsulated bioactive components to the appropriate site of action within the human body. Consequently, it is necessary to understand the potential biological fate of delivery systems within the human gastrointestinal tract. Initial screening experiments of delivery systems are usually carried out using *in vitro* digestion models designed to simulate the human digestive system. These *in vitro* methods have been used to evaluate the digestibility and bioaccessibility of a range of micro-nutrients from different food matrices [10-12]. Recently, *in vitro* digestion models have been used to better understand the behaviour of oil bodies under gastrointestinal conditions [13-15]. These studies have shown that there are appreciable changes in the interfacial composition, aggregation, and structural organization of oil bodies as they pass through different regions of simulated gastrointestinal tracts.

The composition and structure of oil bodies isolated from plant seeds depends on the nature of the isolation procedure used, *e.g.,* temperature, shear, solvent type, and additive type. Oil bodies consist of a triacylglycerol (TAG) core that is coated by a layer of phospholipids and intrinsic proteins (oleosins). However, they may also contain varying amounts of extraneous proteins e.g. seed storage proteins, that are more loosely attached to the oil body surfaces depending on the isolation procedure. Previously, we studied the *in vitro* digestibility and bioaccessibility of fatty acids and α-tocopherol from sunflower urea-washed oil body suspensions [16]. Washing a crude preparation of oil bodies with urea or sodium bicarbonate removes the extraneous proteins that normally surround oil bodies, but leaves the intrinsic proteins in place. If oil bodies were used in food formulations they would probably be in a crude state (*i.e.* the preparation would contain both intrinsic and extraneous proteins). In addition, food formulations often contain various other proteins that could interact with the surfaces of oil bodies and alter their surface chemistry. Slowing down the rate of oil droplet digestion can promote satiety, a physiological target for reducing total food intake; the rate of digestion of emulsified lipids is known to depend on the presence of proteins adsorbed to their surfaces, since this influences the accessibility of lipase to the droplet surfaces [17-18]. The purpose of this study was therefore to establish if some

143   commonly consumed proteins can protect oil bodies under simulated gastrointestinal conditions. The dairy

144   proteins selected for study are common in the diet and have very distinct interfacial properties that represent

145   the behaviour of a range of protein types in aqueous solution.

2. Materials and methods

2.1 Materials

148   Dehulled sunflower seeds (high oleate) were purchased from Cargill Ltd. (West Fargo, USA). Whey protein

149   isolate was purchased from Myprotein.co.uk. (Cheshire, UK). Sodium caseinate was a gift from industry. Both

150   the whey protein and sodium caseinate powders were over 90% protein, and only 0.25% fat, and 0.17%

151   carbohydrate; the rest of the powder was tightly adsorbed water and ash/minerals. Porcine pepsin (#P7125,

152   activity = 650 units/mg of protein calculated using haemoglobin as substrate), porcine pancreatic extract

153   (#L3126, lipase activity = 53 units/mg of powder calculated using tributyrin as substrate, and trypsin activity =

154   2.3 units/mg of powder calculated using TAME (p-tolune-sulfonyl-L-arginine methyl esteras substrate),

155   porcine co-lipase and porcine bile extract (#B8631, contains glycine, taurine, conjugates of hydroxycholic

156   acid) were purchased from Sigma Chemical Company (Dorset, UK.). Gastric lipase analogue of fungal origin

157   (F-AP15, activity >150 units/mg) was obtained from Amano Enzyme Inc. (Nagoya, Japan). All chemicals

158   used for SDS-PAGE analysis were purchased from Bio-Rad (Hercules, USA). Unless otherwise stated, all

159   reagents used were of analytical grade.

2.2 Recovery and purification of oil bodies

161   Oil bodies from sunflower seeds were extracted and purified/washed by the method of Beisson et al (2001) [19]

162   with slight modifications. Sunflower seeds (20g) were kibbled with liquid nitrogen using coffee grinder

163   (DeLonghi KG40, UK) for 30 seconds. The ground seeds were then added to 200 ml of 0.1M Tris-HCl buffer

164   (pH 8) containing 1mM EDTA, and immediately homogenised by a Silverson (L5M, Chesham, UK) at 6000

165   rpm for 40 seconds. The slurry was filtered through 1 layer of Miracloth and the filtrate centrifuged at 10,400

166   g (Beckman Coulter J2-21M, Buckinghamshire, UK) for 20 mins at 4°C. The oil body pad was removed from

167   the surface and placed into a clean bottle; these oil bodies produced were classed as the crude oil bodies

168   (COB) and stored until use at 4 ˚C.

169   Washed oil bodies (WOB) were obtained by re-suspending the crude oil body pad in 200 ml of a 0.1M

170   NaHCO$_3$, 1mM EDTA solution by using a Silverson at 6000 rpm for 10 seconds. The mixture was centrifuged

171   as described above. The upper layer was isolated and washed with 200 ml of a 0.1M NaHCO$_3$, 1mM EDTA

172   solution as described above. The isolated upper layer was then washed twice with 1mM Tris-HCl buffer (pH

173   8) containing 1mM EDTA. The oil body pad was stored at 4°C until use.

2.3 Proximate composition of purified oil body preparations

175   The moisture content of the oil body cream was determined gravimetrically following vacuum drying at 50°C

176   for 24 h. The lipid content of the dried oil body preparation (ca. 0.5-1g) was determined gravimetrically using

177   repeated extraction (3 times in total) with isooctane [9]. The protein content of the defatted dried oil bodies was

178   determined using the BCA (bichinconinic acid) assay [20] following solubilisation of proteins in 2% sodium

179   dodecyl sulfate (SDS) solution at 90°C. Bovine serum albumin was used as a protein standard.

180   **2.4 Preparation of emulsions**

181   **Sunflower seed oil body emulsion**

182   Oil body emulsions were prepared by mixing oil body pad with dH_2O to achieve a 5% emulsion based on the

183   total lipid content. A uniform dispersion of oil bodies was achieved by passing the mixture 10 times through a

184   Potter Elvenheim Homogeniser (Wheaton, USA) at 500 rpm. The emulsion was prepared no longer than 5

185   hours before use.

186   **Protein enriched oil body emulsion**

187   To formulate oil body emulsions at 5% w/v of oil and 1% w/v of protein, WPI or SC was used as protein

188   source for the emulsions. WPI or SC was added into the prepared oil body emulsions. The mixtures were

189   stirred with magnetic stirrer at 100 rpm for 10 minutes. Emulsions were used within 1 hour of formation.

190   **2.5 *In vitro* digestion model**

191   The *in vitro* digestion model was modified from Beysseriat et al.[21] Mun et al.[22] Mandalari et al. [23] and White et

192   al. [16].

193   **Gastric model**

194   The prepared emulsions (20 ml) were placed into 50 ml amber bottles, and the pH was adjusted to 2.5 with a

195   few drops of 1M HCl. NaCl (solid) was added to make a final concentration of 0.15 M; this was followed by

196   adding pepsin and a gastric lipase analogue to the system. Final concentrations of the mixtures were, 146

197   units/ml pepsin and 84 units/ml gastric lipase analogue. The samples were then incubated for 2 hours at 37°C

198   in the incubator and stirred using a magnetic stirrer at 130 rpm.

199   **Duodenal model**

200   The gastric mixture was carried forwarded to the duodenal model. The pH of the samples was immediately

201   adjusted to 5 by adding a few drops of 0.9 M $NaHCO_3$. Bile extract was then added to the system. The

202   samples were then adjusted to pH 6.5 with 0.9 M $NaHCO_3$ (if needed), followed by the addition of pancreatic

203   lipase and co-lipase. Final concentrations of constituents were 4.4 mg/ml bile extract; 54 units/ml pancreatic

204   lipase and 3.2 µg/ml co-lipase. The duodenal digestion then proceeded for 2 hours at 37°C in the incubator and

205   stirred using a magnetic stirrer at 130 rpm.

206 The samples were examined every hour during 4 hours of digestion. The 'before' and 'after' digestion samples
207 were assessed by size analysis, light microscopy, and ζ-potential.

208

209 **2.6 Particle size analysis**

210 Emulsion droplet diameter were determined by using a laser light scattering instrument (LS 13 320 Laser
211 Diffraction Particle Size Analyzer, Beckman Coulter, Inc., USA). Samples (1 ml) were introduced into the
212 universal liquid module, and obscuration was maintained at 7% for all samples by dilution with dH_2O. The
213 diffraction data were analysed using the Fraunhofer diffraction method. Particles with diameters between 0.3
214 to 2000 μm were detected. The fundamental size distribution derived from this technique is volume based i.e.
215 reported percentage distribution within a given size category infers the percentage of the total volume of
216 particles in the entire distribution. The particle size measurements are hereby reported as the volume mean
217 diameter: $d_{4,3} = \sum n_i d_i^4 / \sum n_i d_i^3$, where n_i is the number of droplets of diameter d_i. Each individual particle size
218 measurement was determined from the average of three readings made per sample.

219

220 **2.7 Zeta Potential measurements**

221 Oil body emulsions were diluted in dH_2O to 0.25% (lipid weight). Diluted emulsions were then injected into
222 the measurement chamber of a particle electrophoresis instrument (Delsa Nano C Particle Analyzer, Beckman
223 Coulter, Inc., USA). The instrument settings used were: temperature = $25^{\circ}C$; refractive index of dispersant =
224 1.330; viscosity of dispersant = 0.891 mPa s; relative dielectric constant of dispersant = 79.0; electrode
225 spacing = 50.0 mm. The zeta potential (ζ-potential) was then determined by measuring the direction and
226 velocity of the droplets in an applied electric field from which ζ-potential was calculated using Beckman
227 Software. Each ζ-potential measurement was reported as the average of three readings made per sample.

228

229 **2.8 Imaging Oil Droplets**

230 **2.8.1 Confocal microscopy**
231 A Leica SP5 confocal laser scanning microscope (Leica Microsystems, UK) was used to examine the
232 microstructure of lipid droplets. Proteins were stained with Nile blue (Sigma) (2 μl of 0.01% w/v dye in 75%
233 glycerol were added to 100 μl emulsion) and lipids were stained with Nile red (Sigma) (4 μl of a 0.002% w/v
234 dye in 100% polyethylene glycol were added to 100 μl of emulsion). Stained emulsion (8 μl) was transferred
235 on a glass slide and covered with a glass coverslip (size 18 mm × 18 mm). Nile red was excited using the 514
236 nm line of an Argon laser and Nile blue was excited using the 633 nm line of a Helium-Neon laser.

237 Fluorescence intensity data were collected between 560 to 600 nm for Nile red and 650 to 680 nm for Nile

238 blue. To avoid interference due to cross fluorescence, the two emission spectra were collected using the

239 sequential line scanning mode. Images were processed using the Leica SP5 Image Analysis software and

240 figures were created using Microsoft PowerPoint 2007 (Microsoft Corporation, Redmond, USA).

241

242 **2.8.2 Light Microspcopy**

243 The microstructure of the lipid droplets was determined using optical microscopy (Nikon microscope Eclipse

244 E400, Nikon Corporation, Japan). A drop of the emulsion was placed on a glass slide and cover with a cover

245 slip. The prepared glass slide was observed under the microscope at a magnification of 40x magnification. The

246 images were recorded to observe the change in the microstructure of the samples during digestion**.**

247

248 **2.9 Protein analysis**

249 Protein concentration was determined using the BCA method and equal concentrations of protein samples

250 (20μl) were mixed with 20 µl of sample buffer (Laemmli buffer (Biorad, UK) + 5% β-mercaptoethanol), and

251 heated at 95°C for 5 min then cooled on ice. Proteins were resolved by SDS-PAGE using 4-20%

252 polyacrylamide gels (Mini-Protean TGX Gels, 15- well, 15 µl, Bio-Rad, Hercules, USA) ; gels were

253 positioned within a SE 600 BioRad separation unit and suspended in tank buffer (25 mM Tris, 250 mM

254 Glycine, 0.1% SDS, pH 8.3). Electrophoresis was run at 100 V for 40 min. After electrophoresis, the gel was

255 washed (15 min) once with distilled water then stained (1 hour) with the Imperial Protein Stain (Pierce,

256 Rockford, IL, USA) and destained (8 hours) four times with distilled water. Gels were imaged using a BIO-

257 RAD GS-800 densitometer and images were processed using PDQuest Quantity-one (Bio-Rad, Hercules,

258 USA). Incubation samples were centrifuged (as described above) to isolate the oil droplets (buoyant fraction)

259 from the micellar phase, prior to protein extraction and analysis.

260

261 **2.10 Displacement of intrinsic oil body proteins with bile salts**

262 To analyse the displacement of oleosin on the surface of oil bodies with bile salts, a crude oil body emulsion

263 was subjected to *in vitro* duodenal digestion conditions as described above, but no enzymes, only bile extract

264 was added into the system, and a control was included in this experiment, where 20ml of crude oil bodies

265 emulsion was incubated at 37°C for 2 hours. Incubation samples were centrifuged (as described above) to

266 isolate the oil droplets (buoyant fraction) from the micellar phase, prior to protein extraction and analysis.

267

268 **2.11 Calculation and Statistical analysis**

269　All experiments were carried out on triplicate emulsion preparations; statistical analysis was performed by
270　one-way ANOVA and Least Significant Different (LSD) using SPSS 15.0. Assessment of significance was
271　based on a 95% confident limit (P<0.05). Values are expressed as means ± SD.

272　**3. Results and discussion**

273　**3.1 Characterisation of oil body-based emulsion droplets during digestion**

274　Confocal analysis of WOB and protein enriched WOB preparations, was carried out to make sure that the
275　extra dairy proteins were physically associated with the WOB surface. Figure 1 shows the location of lipid
276　(green) and that of the proteins (red). Frome these images we can see that WOBs are surrounded by a thin
277　layer of protein, this layer appears to increase in thickness on adding WPI or SC, indicating an association
278　between these added proteins and the surface of the washed oil bodies. Addition of SC appears to generate the
279　thickest protein shell.

280　The composition of the crude oil bodies recovered in this study was approximately 76.2 ± 7.6 % lipid and 17.5
281　± 0.9 % protein (dry weight). The composition of the washed oil bodies was approximately 89.0 ± 9.6 % lipid
282　and 3.9 ± 0.8 % protein (dry weight). The ζ-potential of crude oil bodies (COB), washed oil bodies (WOB),
283　whey protein isolate-enriched oil bodies (WOB-WPI) and sodium caseinate-enriched oil bodies (WOB-SC) at
284　pH 6.5 were -37.4 ± 8.9, -17.9 ± 4.1, -37.8 ± 1.2 and -59 ± 1.9 mV, respectively (Figure 2). The negative
285　surface charge on oil bodies can be attributed to the interface consisting of anionic phospholipids[24] and protein
286　molecules that were above their isoelectric point at this pH. After adding WPI and SC to WOB, there was a
287　significant increase (P<0.05) in the negative charge of the oil bodies. This can be explained by WPI and SC
288　adsorbing onto the oil body surfaces thereby increasing their negative charge. Interestingly, the SDS-PAGE
289　profiles of proteins from the protein-enriched washed oil bodies (Figure 8) show that WPI and SC become
290　associated with WOBs, which is consistent with the our deductions from the surface charge data and from the
291　confocal images..

292　The pattern of ζ-potential changes of oil body and protein-enriched oil bodies was similar during digestion.
293　Under gastric conditions (first 2 h) at pH 2.5, the ζ-potential of COB, WOB, WOB-WPI and WOB-SC
294　emulsion droplets changed from negative to positive (+7.0 ± 1.8, +24.9 ± 3.0, +41.7 ± 4.4 and +30.0 ± 0.8
295　mV, respectively). All emulsion droplets remained positively charged for 2 h during incubation in the gastric
296　model. The charge on the oil droplets after digestion in the small intestine became strongly negative: -54.5 ±
297　8.1, -70.7 ± 20.9 -86.3 ± 3.0 and -78.7 ± 6.4 mV, respectively. Interestingly, the charge associated with the
298　surface of the COB derived droplets in the duodenal conditions was lower than the charge associated with the
299　surface of the droplets in the other oil body-based emulsion preparations. This suggests that the association of
300　bile salts with the surface of the crude oil bodies (and the commensurate displacement of surface proteins)
301　appears less extensive for this case than for the other oil bodies.

302   The particle size distribution and optical microscopy images of all oil bodies (COB, WOB, WOB-WPI and

303   WOB-SC) pre- and post-incubation in the *in vitro* gastric model can be seen in Figures 3 to 6. Each oil body

304   emulsion contained droplets of a similar size prior to digestion, but thereafter, significant changes occurred.

305   The mean particle diameters ($d_{4,3}$) of the WOB, WOB-WPI and WOB-SC emulsion droplets (3.2 ± 0.6, 3.9 ±

306   1.0 and 2.6 ± 0.1 µm, respectively) were significantly smaller (P<0.05) than COB (5.6 ± 1.4 µm) prior to

307   incubation in the gastrointestinal model (Figure 7). During gastric digestion for 2 hours the diameter ($d_{4,3}$) of

308   all emulsion droplets appeared to increase significantly. After 2 hours digestion in the gastric model followed

309   by two hours incubation in the duodenal model the mean diameter of the particles in the COB emulsions (37.2

310   ± 26.7 µm) was slightly decreased from gastric model (p>0.05). However, WOB-SC emulsion droplets (7.8 ±

311   2.4 µm) decreased significantly (P<0.05), whereas WOB and WOB-WPI emulsion droplets (104.7 ± 24.3 and

312   56.9 ± 16.2 µm, respectively) increased significantly in size (P<0.05). In addition, when digested in duodenal

313   conditions, a shift from a mono-modal distribution to a bi-modal distribution was observed for COB, but not

314   for the other emulsions. The presence of several peaks in the particle size distribution interferes with the

315   measurement of the mean particle diameter of the lipid droplets during digestion. The relatively large standard

316   deviations observed in the particle size distributions are typical of measurements made in highly aggregated

317   emulsion systems and are usually attributed to changes in sample structure induced by dilution and stirring

318   within the light scattering instrument [22].

319   The particle size analyser cannot distinguish between aggregation and coalescence, and so microscopic

320   observation of the oil body suspensions was carried out to provide further evidence of structural changes. The

321   optical microscopy images revealed changes in system microstructure during incubation in the gastric model.

322   The oil bodies in the COB, WOB-WPI and WOB-SC emulsions were seen to flocculate during the first hour

323   of incubation and then coalesce during the second hour, whereas there was already some coalescence evident

324   during the first hour of incubation in the WOB emulsions. Under duodenal conditions, free oil droplets were

325   clearly observed in WOB and WOB-WPI whereas few free oil droplets were observed in COB and WOB-SC.

326   These observations explain the shift in the particle size data for all emulsions. From these results we can see

327   that in our model system COB behaves similarly to WOB-SC, but there is a marked contrast when compared

328   with WOB and WOB-WPI.

329   Wu and co-workers (2012)[13] demonstrated the partial protective effect of carrageenan at the surface of

330   soybean oil bodies against digestion. Similar to our work, they observed a change in the surface charge of oil

331   bodies during incubation, with a significant negative charge (-70 mV) in the presence of bile salts. This

332   suggests that bile salts associate with the surface of these droplets, either through direct physical association or

333   through displacement of some of the surface material. Their surface area-weighted particle size data ($d_{3,2}$)

334   suggests that their soybean oil body preparations varied in size that did not change radically during the gastric

335   phase, then developed a broader distribution during the duodenal phase. Micrographs of the same material told

336   a slightly different story with a significant increase in particle size during the gastric phase, this increase being

337   inversely proportional to the amount of carrageenan that was present; the droplets then decreased in size

338   during the duodenal phase. The increase in droplet size under gastric conditions coincided with the loss of

339   oleosin, presumably through the action of pepsin, which was inhibited in the presence of carrageenan.

340   In a study of the digestion of almond seed oil bodies, Gallier and Singh[14] observed that the oil bodies

341   aggregated and coalesced under gastric conditions. During the duodenal phase the measured change in particle

342   size depended on the mode of measurement. The surface area-weighted values $d_{3,2}$ revealed a reduction in

343   average diameter from 20 μm (immediately after the gastric phase) to 5 μm after 15 minutes and until the

344   endpoint at 120 minutes. On the other hand, $d_{4,3}$ values revealed an unchanged average diameter for the first

345   60 minutes of duodenal conditions, followed by a gradual increase to almost 45 μm after a total duodenal

346   incubation of 120 minutes. This is consistent with our data where we used the volume-weighted measure of

347   the average particle size of oil droplets. The change that they have reported in the zeta potential of almond

348   seed oil bodies reflects the change we have seen with our sunflower seed oil bodies. The charge of their

349   almond oil bodies was less than +10 mV after 60 and 120 minutes under gastric conditions, followed by a

350   gradual change in charge to almost -50 mV after 45 minutes, presumably due to the uptake of bile salts under

351   duodenal conditions. Similar effects of bile salts on the surface charge of protein-stabilised emulsion droplets

352   have been reported [25-27]. Mun et al [22] studied the changes in the droplet size of emulsions formed with whey

353   proteins compared to an emulsion formed with caseinate after *in vitro* hydrolysis by pancreatic lipase at pH 7.

354   They reported that in their conditions whey protein isolate emulsions are the least stable. Based on

355   microscopic observations, the caseinate stabilised emulsions were more prone to flocculation rather than

356   coalescence whereas the whey protein stabilised emulsions were highly prone to coalescence, which is

357   consistent with our observations.

358   WPI and SC are milk proteins commonly used as food ingredients because of their surface active properties.

359   Whey protein and caseinate produce an interfacial film with different properties [28], notably with different

360   adsorption and surface rheological behaviours [29, 30]. In brief, the globular β-lactoglobulin forms a highly elastic

361   interfacial film, whereas β-casein forms a weaker interfacial film, but the charged N-terminal region provides

362   excellent steric stabilization. In other words, β-casein is a flexible/'soft' protein, which changes its

363   conformation more easily than β-lactoglobulin which is a 'hard', globular protein [31]. As a consequence, β-

364   casein can be displaced from an interface much more readily than β-lactoglobulin. This rule of thumb is

365   clearly less reliable in a system complicated by enzymic action and pH changes.

366   Oil droplets were recovered from the incubation systems by centrifugation, just after the gastric and

367   duodenal phases. The proteins still associated with their surfaces were studied by SDS-PAGE (Figure 8). Loss

368   of bands indicates removal of proteins from the surface, and/or digestion (full or partial); new bands indicate

369   remnant protein fragments, left behind after partial protein digestion, which remain associated with the droplet

370 surface. For the oil bodies, the loss of the oleosin band (~18-21 kDa) during digestion in the gastric model, and

371 the appearance of protein fragments either between 6.7 and 17.5 kDa, or less than 6.7 kDa, indicates the

372 breakdown of oleosin into small peptides that appear to remain bound to/associated with the oil droplets.

373 Oleosin has three functional motifs: an amphipathic N-terminal region, a central hydrophobic antiparallel β-

374 strand domain and an amphipathic C-terminal domain with variable length[2]. It is likely that the protruding part

375 of the oleosin molecule, which provides a strengthened layer on the surface, is susceptible to enzymatic

376 cleavage and leads to the weakening and consequential coalescence of oil bodies. Pepsin hydrolyses peptide

377 bonds at the N-terminus of aromatic residues [32]. Given the amino acid sequence of oleosin protein in sunflower

378 seed, there are eleven potential sites of pepsin action, and 4 of these peptide bonds are within the exposed

379 domains of oleosin on the surface of oil bodies [33-35].

380 Qualitative examination of protein molecular weights in COB reveals a general degradation of proteins

381 resulting in an increase in the number of bands between 6.7 to 17.5 kDa after incubation in the gastric model

382 (lane B and C). The major band in this region has been highlighted with a green box in Figure 8; this band

383 may represent the hydrophobic domain (and associated residual hydrophilic domain 'stumps') of oleosin, left

384 behind securely anchored in the oil phase after the action of pepsin on the exposed hydrophilic domains.

385 One unique feature of the COB data is that some 'complete' oleosin also appears to remain after the initial

386 gastric phase of digestion. Perhaps the extraneous proteins (that we have already suggested shield the surface

387 of the oil bodies and so affect the apparent surface charge), protect exposed oleosin domains from digestion to

388 some extent. It could be argued that a similar protection of oleosin is afforded by extraneous almond proteins

389 during gastric incubation [14]. This shielding from enzyme activity is not apparent for WPI and SC enriched

390 WOB material. Interestingly, protein breakdown was much more efficient in the WOB emulsion as no protein

391 bands were seen on the protein gel after the gastric conditions (2 hours). This suggests that all the proteins

392 were degraded and/or removed from the surface of the droplets (compare lane E with lane F). It is worth

393 noting that the WOB material used for this study contained a protein, not observed in the parent COB material,

394 that coincides with the putative 'oleosin hydrophobic domain' band. This protein fragment may be present on

395 all the parent COB and WOB samples (or is an artefact of sample preparation for SDS-PAGE analysis), but is

396 only observed when its loading concentration effectively increases through removing extraneous proteins

397 during the oil body washing phase, **or** some proteolytic activity was present in the sample (perhaps due to an

398 endogenous enzyme). If the latter explanation is correct, then one may speculate that if the COB material is

399 left for any time (even chilled) before washing, then such a transformation may be possible.

400 For both WOB-WPI and WOB-SC emulsions (lanes H and I and lanes K and L) incubation in the gastric

401 model resulted in a general protein breakdown/loss, but less dramatic compared with WOB, as protein bands

402 are still clearly visible (lanes I and L). This is even more marked in WOB-WPI compared with WOB-SC. As

403 was the case for COB emulsions, there is a suggestion that after the gastric phase, the exposed domains of

404 oleosin in these protein-enriched WOB emulsions have been removed through digestion, leaving a residual

405 protein composed predominantly of the hydrophobic domain. Protein breakdown/loss continued for all the

406 emulsions with a clear reduction in the molecular weight of all the remaining peptides (lane D, G, J and M). In

407 the case of WOB-WPI, it is possible that after 2 hours under gastric conditions some β-lactoglobulin remains

408 intact, but its molecular weight coincides with one of the oleosin isoforms, so it is not possible, with the

409 current data, to stipulate categorically whether at least a proportion of one or the other protein (or both) survive

410 the gastric phase; taken overall, the SDS-PAGE data provides a stronger case for the retention of some of the

411 β-lactoglobulin.

412 Whey protein is a complex mixture of different proteins: ca. 55% β-lactoglobulin (18.4 kDa), 24% α-

413 lactalbumin (14.2 kDa), 5% serum albumin (66.2 kDa) and 15% immunoglobulins (90 kDa). SDS-PAGE (lane

414 I) of WOB-WPI digested in the gastric model, suggest breakdown/loss of α-lactalbumin but possible retention

415 of the β-lactoglobulin protein under these conditions, implying specificity of the action of the pepsin enzyme.

416 This breakdown of protein in WPI is consistent with previous studies [13, 36-38]. Beta-lactoglobulin in its native

417 form has indeed been recognised to be resistant to hydrolysis in the gastric phase [39]. However, when a change

418 in conformation occurs, such as during adsorption to the oil-water interface, the protein becomes susceptible to

419 pepsin hydrolysis [38]. For WOB-SC, sodium caseinate contains the four main caseins; β-casein (23 kDa), $α_{s1}$-

420 casein (24 kDa), $α_{s2}$-casein (25 kDa) and κ-casein (19 kDa) in the ratios 3:4:1:1, respectively. However, the

421 commercial SC was mainly composed of polypeptides with their MW within range of 29.4 to 37.6 kDa (lane

422 K). This was slightly higher than the MW of caseins (19-25 kDa) due to the polymerization of proteins during

423 commercial processing. SDS-PAGE (lane L) of WOB-SC digested in the gastric model, suggest complete

424 breakdown of oleosin in WOB and all polypeptides in SC. This breakdown of caseins by protein hydrolysis in

425 gastric conditions is in agreement with the previous studies [40-42].

426 Finally, there is a clear reduction in the intensity of protein bands in all emulsions after the duodenal

427 digestion (lane D, G, J and M). This confirms the presence of active proteases in the porcine pancreatic

428 extract. This agrees with Singh et al. [43] who reported that commercial pancreatic lipase from Sigma-Aldrich

429 company causes the breakdown of protein in a β-lactoglobulin-stabilised emulsion.

430 **3.2 Protein composition of oil bodies after treatment with bile salts**

431 As mentioned earlier, the dominant intrinsic protein associated with the surfaces of the oil bodies are the

432 oleosins [3, 44]. Oleosins from diverse species range in molecular weight (MW) from approximately 15 to 26 kDa

433 [44]. The exact sizes of the different isoforms vary from one plant to another, for example 16 and 18 kDa in

434 maize, 18 and 24 kDa in soybean and 18 and 21 kDa in sunflower seeds [45]. Work was carried out to establish if

435 bile salts were capable of displacing oleosin from a preparation of crude oil bodies. Bile salts can absorb onto

436 and remove other materials e.g. proteins and emulsifier from the lipid surface [17]. Maldonado-Valderrama et al.

Food & Function

437   [18] reported that the bile salts can almost completely displace the intact protein β-lactoglobulin network under

438   duodenal conditions. It is not yet known if intrinsic oil body proteins are displaced by bile salts or not. Figure

439   9 shows the protein profile of the micellar phase removed after incubation of crude oil bodies (COB) with bile

440   salts (lane E). This profile is similar to the protein profile of the control COB (no bile salts) after 2 h

441   incubation but before phase separation (lane C); whereas there were only a few proteins in the micellar phase

442   of the COB control after incubation (lane D). These results suggests that almost all the surface proteins of oil

443   bodies, including oleosin, were displaced by bile salts. Interestingly, the data also show that the pattern of

444   protein bands in COB control after incubation is similar to the pre-incubation profile (lane C compared to lane

445   B). However, there are small molecular weight protein bands (between 6.7 and 17.5 kDa) accumulating in the

446   COB control after incubation (lane C). This observation suggests that there is some breakdown of proteins in

447   this sample; the crude oil body preparation may contain some carry-over enzymes with proteolytic activity, but

448   this effect seems almost negligible. These results show the potential of bile salts to displace proteins at the

449   surface of oil bodies, even well-anchored proteins such as oleosin. Whether bile salts could effect this

450   displacement if oleosin was reduced to the hydrophobic domain after gastric digestion is not clear from this

451   work; it has been suggested that such a remnant, if it exists, could affect the rate of lipase digestion in the

452   duodenum [14].

4. Conclusions

454   Sunflower seed oil bodies have the capacity to associate with extraneous proteins including whey protein

455   isolates and casein proteins. This extraneous protein environment surrounding oil bodies affects the apparent

456   surface charge and stability of oil bodies, which may have important consequences for the commercial

457   application of oil bodies as delivery systems in foods. The proteins associated with the surface of the

458   sunflower oils bodies studied (crude, or washed, or washed and enriched with WPI or casein) are, to a greater

459   or lesser extent, hydrolysed and/or removed from the surface during simulation of gastro-intestinal conditions,

460   causing significant changes in the morphology of the droplets. Sunflower seed proteins not intrinsic to oil

461   bodies (present in COB), and caseinate (present in WOB-SC) both appear to cause flocculation of droplets in

462   the gastric phase, whereas WOB and WOB-WPI display more coalescence than flocculation at this stage.

463   Although it is clear that bile salts dominate the surface of all the droplets in the duodenal phase of digestion,

464   COB and WOB-SC yield smaller droplets in the duodenal phase of the digestion model employed, compared

465   with WOB or WOB-WPI. This may have an effect on the rate of triacylglycerol digestion. The reason for

466   these differences in droplet size is not entirely clear, but is should be pointed out that the competing dynamics

467   of bile salt insertion into the surface of the droplets emerging from the gastric phase, and their tendency to

468   coalesce will affect the size of the droplets throughout that phase. We have evidence that bile salts are able to

469   displace oleosin. It may therefore be possible that the extraneous seed proteins are protecting the oleosin

470   during the gastric phase, thus restricting the droplet size during bile salt insertion. These results may have

471   important implications for the design of functional food products that control the digestion and release of

472   lipids from oil body-based delivery systems.

473   **Acknowledgements**

475

476   **References**

477   1.   J. T. C. Tzen, Y. Z. Cao, P. Laurent, C. Ratnayake and A. H. C. Huang, *Plant Physiol.*, 1993, **101**,
478   267-276.

479   2.   J. T. C. Tzen, G. C. Lie and A. H. C. Huang, *J. Biol. Chem.*, 1992, **267**, 15626-15634.

480   3.   J. T. C. Tzen and A. H. C. Huang, *J. Cell Biol.*, 1992, **117**, 327-335.

481   4.   F. Beisson, N. Ferte and G. Noat, *Biochem. J.*, 1996, **317**, 955-956.

482   5.   P. J. E. Thoyts, J. A. Napier, M. Millichip, A. K. Stobart, W. T. Griffiths, A. S. Tatham and P. R.
483   Shewry, *Plant Sci.*, 1996, **118**, 119-125.

484   6.   D. J. Lacey, N. Wellner, F. Beaudoin, J. A. Napier and P. R. Shewry, *Biochem. J.*, 1998, **334**, 469-
485   477.

486   7.   I. D. Fisk, D. A. White, A. Carvalho and D. A. Gray, *J. Am. Oil Chem. Soc.*, 2006, **83**, 341-344.

487   8.   N. Nantiyakul, S. Furse, I.D. Fisk, T.J. Foster, G. Tucker and D.A. Gray, *J. Am. Oil Chem. Soc* **,** 2012,
488   **89** (10) 1867-1872

489   9.   D.A. Gray, G. Payne, D.J. McClements, E.A. Decker and M. Lad , *European Journal of Lipid Science
490   and Technology*, 2010, **112** (7), 741-749

491   10.   D. A. Garrett, M. L. Failla and R. J. Sarama, *J. Agri. Food Chem.*, 1999, **47**, 4301-4309.

492   11.   E. Hedren, V. Diaz and U. Svanberg, *Eur. J. Clin. Nutr.*, 2002, **56**, 425-430.

493   12.   D. D. Miller, B. R. Schricker, R. R. Rasmussen and D. Vancampen, *Am. J. Clin. Nutr.*, 1981, **34**,
494   2248-2256.

495   13.   N. Wu, X. Huang, X.-Q. Yang, J. Guo, S.-W. Yin, X.-T. He, L.-J. Wang, J.-H. Zhu, J.-R. Qi and E.-L.
496   Zheng, *J. Agri. Food Chem.*, 2012, **60**, 1567-1575.

497   14.   S. Gallier and H. Singh, *Food Funct.*, 2012, **3**, 547-555.

498   15.   S. Gallier, H. Tate and H. Singh, *J. Agric. Food Chem.*, 2013, **61**, 410-417.

499   16.   D. A. White, I. D. Fisk, S. Makkhun and D. A. Gray, *J. Agri. Food Chem.*, 2009, **57**, 5720-5726.

500   17.   J. Maldonado-Valderrama, P. Wilde, A. Macierzanka and A. Mackie, *Adv. Colloid Interfac. Sci.*,
501   2011, **165**, 36-46.

502   18.   J. Maldonado-Valderrama, N. C. Woodward, A. P. Gunning, M. J. Ridout, F. A. Husband, A. R.
503   Mackie, V. J. Morris and P. J. Wilde, *Langmuir*, 2008, **24**, 6759-6767.

504   19.   F. Beisson, N. Ferte, R. Voultoury and V. Arondel, *Plant Physiol. Biochem.*, 2001, **39**, 623-630.

505   20.   P. K. Smith, R. I. Krohn, G. T. Hermanson, A. K. Mallia, F. H. Gartner, M. D. Provenzano, E. K.
506   Fujimoto, N. M. Goeke, B. J. Olson and D. C. Klenk, *Anal. Biochem.*, 1985, **150**, 76-85.

507   21.   M. Beysseriat, E. A. Decker and D. J. McClements, *Food Hydrocolloids*, 2006, **20**, 800-809.

508   22.   S. Mun, E. A. Decker and D. J. McClements, *Food Res. Int.*, 2007, **40**, 770-781.

509   23.   G. Mandalari, R. M. Faulks, G. T. Rich, V. Lo Turco, D. R. Picout, R. B. Lo Curto, G. Bisignano, P.
510   Dugo, G. Dugo, K. W. Waldron, P. R. Ellis and M. S. J. Wickham, *J. Agri. Food Chem.*, 2008, **56**,
511   3409-3416.

512   24.   G. Payne, M. Lad, T. Foster, A. Khosla and D.A. Gray, *Colloids and Surfaces B: Biointerfaces*, 2014,
513   **116,** 88-92

514   25.   A. Sarkar, K. K. T. Goth, R. P. Singh and H. Singh, *Food Hydrocolloids*, 2009, **23**, 1563-1569.

515   26.   M. Golding, T. J. Wooster, L. Day, M. Xu, L. Lundin, J. Keogh and P. Clifton, *Soft Matter*, 2011, **7**,
516   3513-3523.

517   27.   J. Li, A. Ye, S. J. Lee and H. Singh, *Food Funct.*, 2012, **3**, 320-326.

518   28.   J. N. de Wit, *J. Dairy Sci.*, 1998, **81**, 597-608.

519   29.   M. Bos and T. van Vliet, *Adv. Colloid Interface Sci.*, 2001, **91**, 437-471.

520   30.   J. R. Mitchell, *Dev. Food Prot*, 1986, **4**, 291-338.

521   31.   T. Arai and W. Norde, *Colloids and Surfaces*, 1990, **51**, 1-15.

522   32.   J. S. Fruton, S. Fujii and M. H. Knappenberger, *P Natl Acad Sci USA*, 1961, **47**, 759-761.

523   33.   J. C. F. Chen and J. T. C. Tzen, *Plant Cell Physiol.*, 2001, **42**, 1245-1252.

524   34.   M. Li, D. J. Murphy, K. H. K. Lee, R. Wilson, L. J. Smith, D. C. Clark and J. Y. Sung, *J. Biol. Chem.*,
525   2002, **277**, 37888-37895.

526   35.   S. Vandana and S. C. Bhatla, *Plant Physiol. Biochem.*, 2006, **44**, 714-723.

527   36.   D. G. Schmidt and B. W. Vanmarkwijk, *Neth. Milk Dairy J.*, 1993, **47**, 15-22.

528   37.   N. Kitabatake and Y. I. Kinekawa, *J. Agric. Food Chem.*, 1998, **46**, 4917-4923.

529   38.   A. Malaki Nik, A. J. Wright and M. Corredig, *J. Colloid Interface Sci.*, 2010, **344**, 372-381.

530   39.   I.M. Reddy, N.K.D. Kella and J.E. Kinsella, *Journal Agric. Food Chem.*, 1988, **36** (4), 737-74138.
531

532   40.   A. Macierzanka, A. I. Sancho, E. N. C. Mills, N. M. Rigby and A. R. Mackie, *Soft Matter*, 2009, **5**,
533   538-550.

534   41.   M. R. Guo, P. F. Fox, A. Flynn and P. S. Kindstedt, *J. Dairy Sci.*, 1995, **78**, 2336-2344.

535   42.   M. Defernez, G. Mandalari and E. N. C. Mills, *Electrophoersis*, 2010, **31**, 2838-2848.

536   43.   H. Singh, A. Ye and D. Horne, *Prog. Lipid Res.*, 2009, **48**, 92-100.

537   44.   A. H. C. Huang, *Annu.Rev. Plant Phys.*, 1992, **43**, 177-200.

538   45.   J. T. C. Tzen, Y. K. Lai, K. L. Chan and A. H. C. Huang, *Plant Physiol*, 1990, **94**, 1282-1289.

539

540

541   **Legends to Figures**

542   **Figure 1.**

543   Confocal Micrographs of WOB (washed oil bodies), WOB-WPI (washed oil bodies + whey protein isolate)
544   and WOB-SC (washed oil bodies + sodium caseinate) prepared as described in the methods section.

545   **Figure 2.**

546   Zeta potential of COB, WOB, WOB-WPI and WOB-SC emulsion; before and during gastrointestinal digestion
547   for 4 hours (1h and 2h in gastric condition, 3h and 4h in duodenal condition).

548

549   **Figure 3.**

550   Particle size distributions (%volume) and light microscopy pictures of COB emulsion before and during
551   gastrointestinal digestion for 4 hours (1h and 2h in gastric condition, 3h and 4h in duodenal condition).

552

553   **Figure 4.**

554   Particle size distributions (%volume) and light microscopy pictures of WOB emulsion before and during
555   gastrointestinal digestion for 4 hours (1h and 2h in gastric condition, 3h and 4h in duodenal condition).

556

557   **Figure 5.**

558   Particle size distributions (%volume) and light microscopy pictures of WOB-WPI enriched emulsion before
559   and during gastrointestinal digestion for 4 hours (1h and 2h in gastric condition, 3h and 4h in duodenal
560   condition).

561

562   **Figure 6.**

563 Particle size distributions (%volume) and light microscopy pictures of WOB-SC enriched emulsion before and
564 during gastrointestinal digestion for 4 hours (1h and 2h in gastric condition, 3h and 4h in duodenal condition).

565

566 **Figure 7.**

567 Mean diameter ($d_{4,3}$) of COB, WOB, WOB-WPI and WOB-SC emulsion before and during gastrointestinal
568 digestion for 4 hours (1h and 2h in gastric condition, 3h and 4h in duodenal condition).

569

570

571 **Figure 8.**

572 SDS-PAGE of proteins associated with COB, WOB, WOB-WPI and WOB-SC droplets before and during
573 gastrointestinal digestion for 4 hours (2 hours in gastric condition followed by 2 hours in duodenal condition)

574 Protein standard marker (lane A); initial COB droplets (lane B); digested COB under gastric conditions (lane
575 C); digested COB under duodenal conditions (lane D); initial WOB droplets (lane E); digested WOB under
576 gastric conditions (lane F); digested WOB under duodenal conditions (lane G); initial WOB-WPI droplets
577 (lane H); digested WOB-WPI under gastric conditions (lane I); digested WOB-WPI under duodenal conditions
578 (lane J); initial WOB-SC droplets (lane K); digested WOB-SC under gastric conditions (lane L); and digested
579 WOB-SC under duodenal conditions (lane M)

580 Red arrows indicate bands the correlate with known molecular weights of specific proteins; the green
581 box highlights a band that may be the hydrophobic domain of the oleosin protein.

582

583 **Figure 9.**

584 SDS-PAGE of proteins in crude oil body (COB) droplets after incubation with bile salts for 2 hours under
585 duodenal conditions (no prior gastric phase)

586 Protein standard marker (lane A); COB pre-incubation (lane B); COB control [no bile salts] (pre-separation
587 into micellar and buoyant (oil droplet) fractions) (lane C); micellar phase of COB control (lane D); and
588 micellar phase of COB after incubation with bile salts (lane E).

589

590 **Figure 1.**

591 WOB
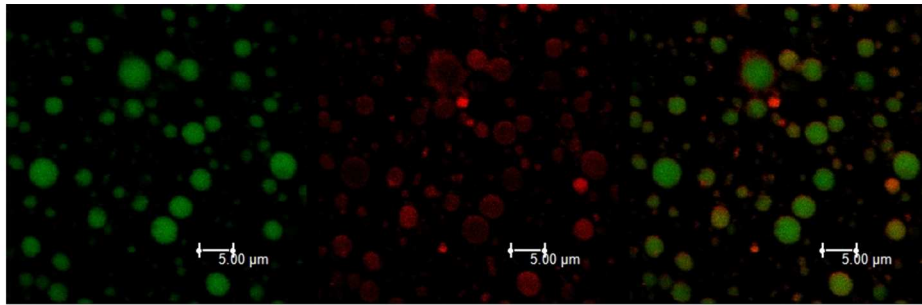
597

598 WOB-WPI
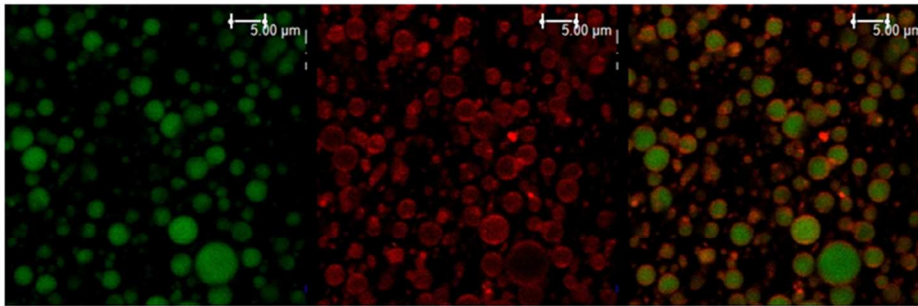
599

600

601 WOB-SC
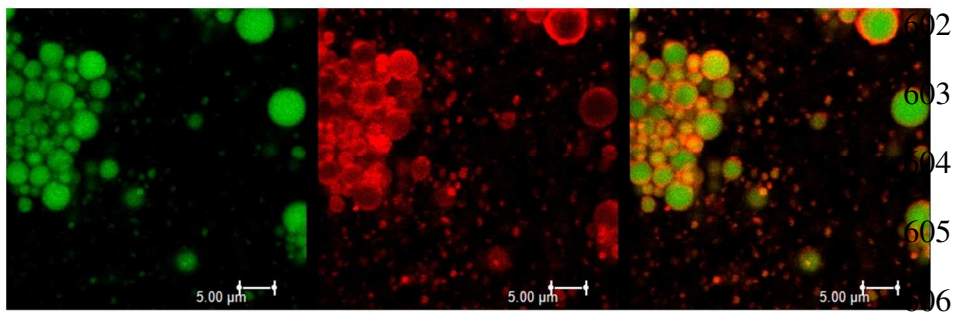
607

608

609 Note: From left to right: lipid stained with Nile red; protein stained with Nile blue; overlay of lipid
610 and protein stained.

611

612　**Figure 2.**
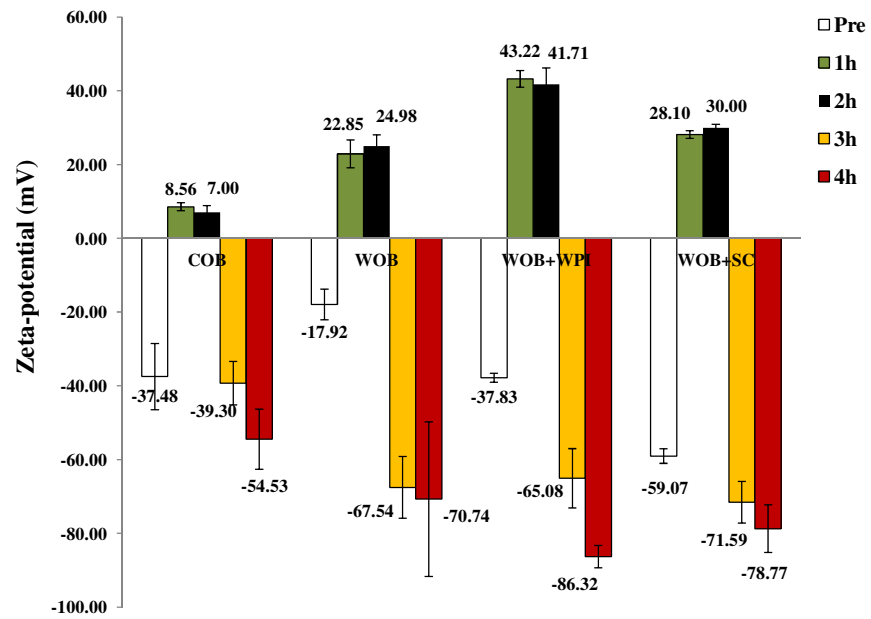
613

614

615

616

617

618

619

620

621

622

623

624

625

626

627

628

629   **Figure 3.**

630
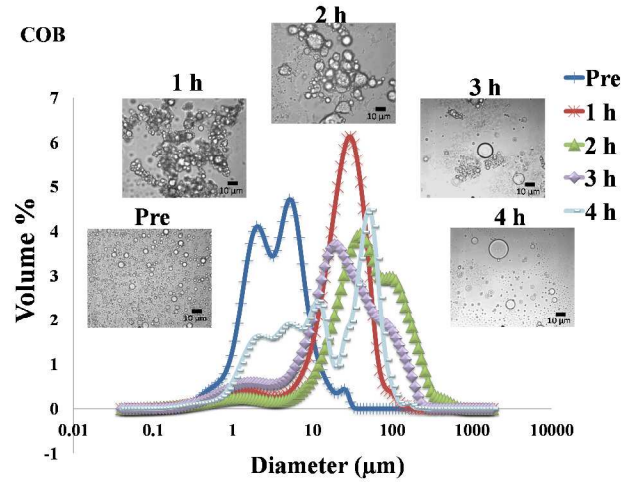
631
632
633
634

635   **Figure 4.**

636
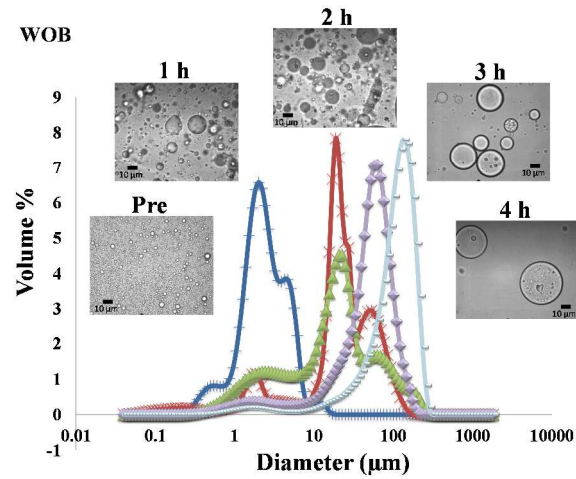
637
638
639

640

641   **Figure 5.**

642
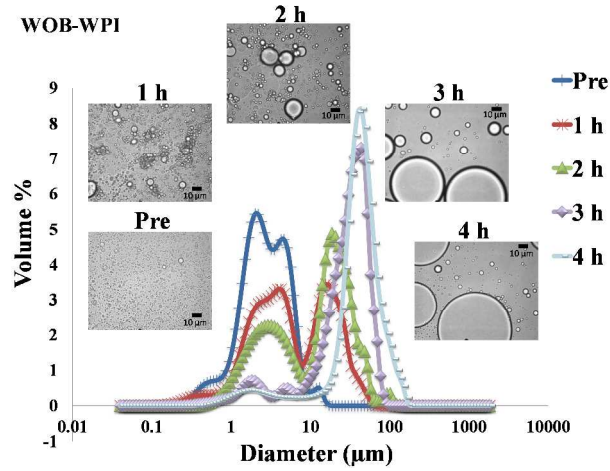
643
644
645

646   **Figure 6.**

647
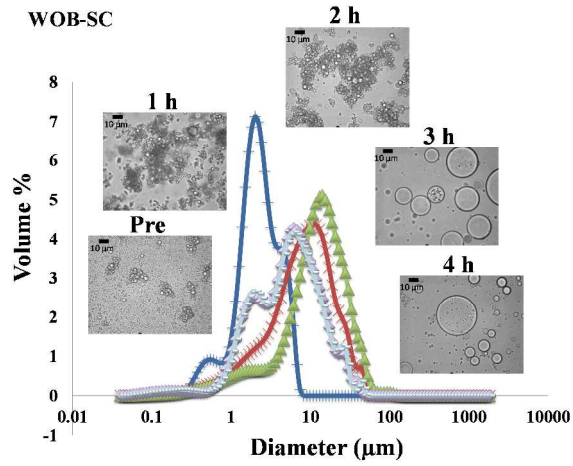
648
649
650
651
652

653

654 **Figure 7.**

655
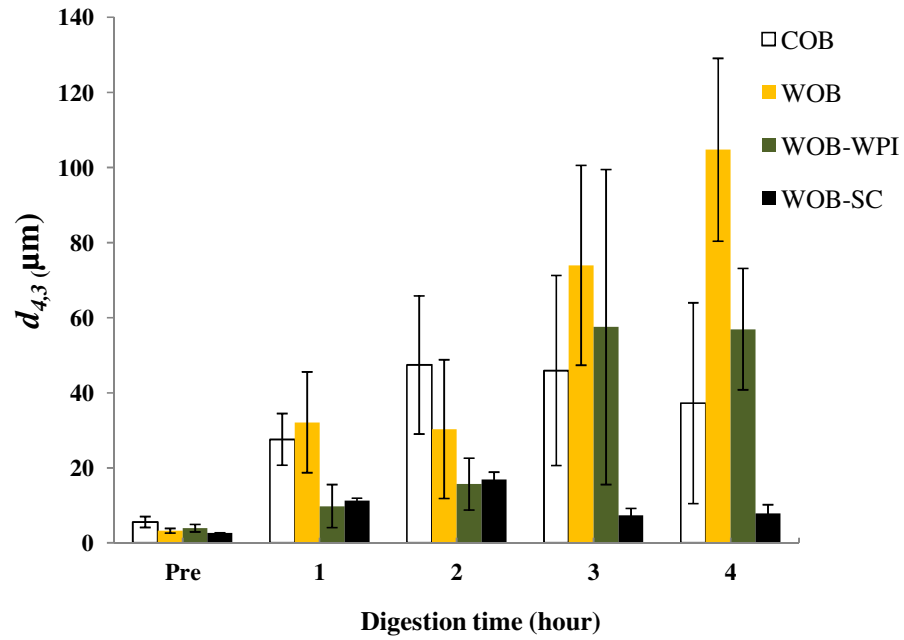
656

657

658

659

660

661

662

663

664

665

666

667

668

669

670

671 **Figure 8.**
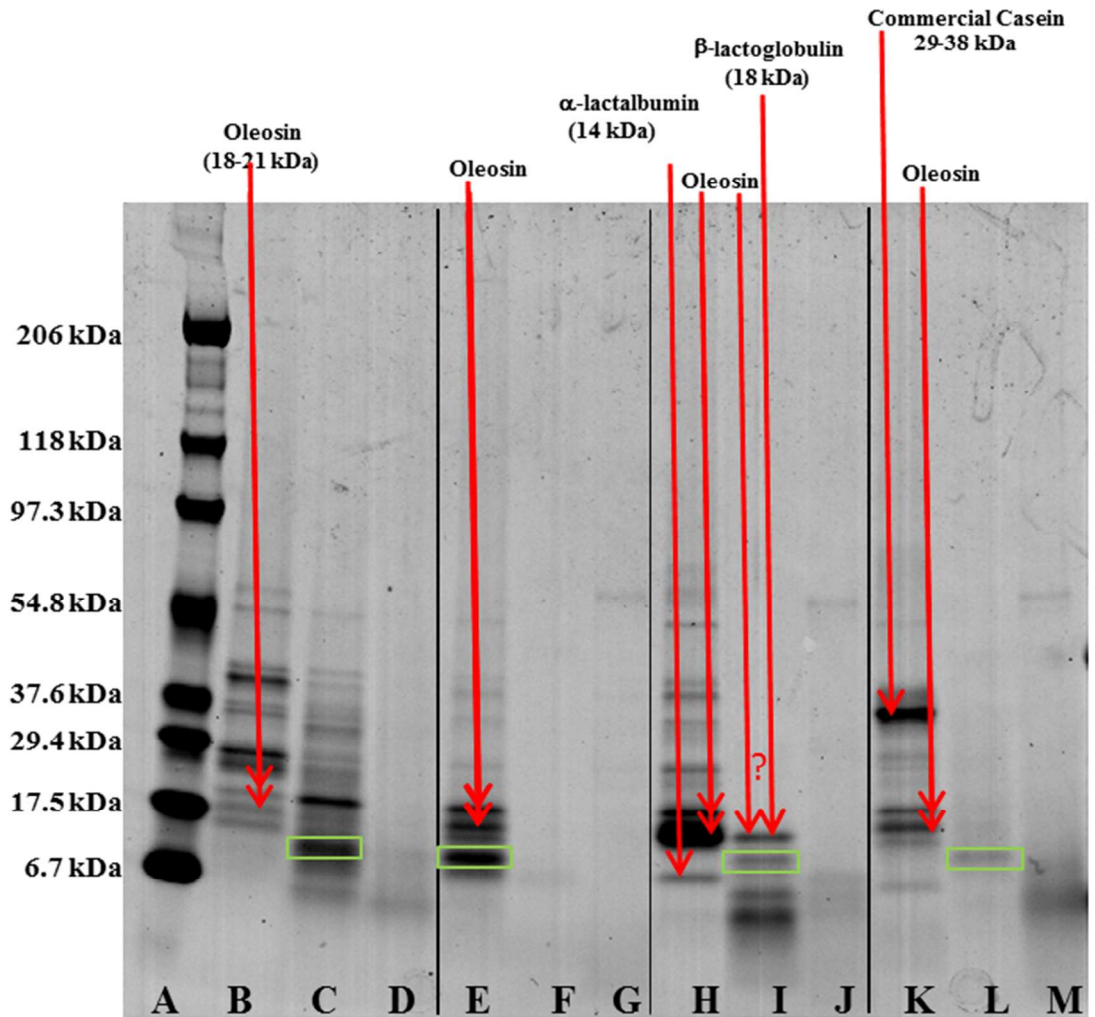
672

673

674

675

676

677   **Figure 9.**

678

679
680
681
682
683
684